Mon. Not. R. Astron. Soc. **394,** 2238–2246 (2009) doi:10.1111/j.1365-2966.2009.14492.x

Non-thermal transient sources from rotating black holes

Maurice H. P. M. van Putten[1]★ and Alok C. Gupta[2]

[1]*Le Studium Institute for Advanced Studies, 3D Avenue Recherche Scientifique, 45071 Orléans Cedex 2, France*
[2]*Aryabhatta Research Institute of Observational Sciences (ARIES), Manora Peak, Nainital 263129, India*

Accepted 2009 January 12. Received 2008 December 21; in original form 2008 November 7

ABSTRACT

Rotating black holes can power the most extreme non-thermal transient sources. They have a long-duration viscous time-scale of spin-down, and produce non-thermal emissions along their spin-axis, powered by a relativistic capillary effect. We report on the discovery of exponential decay in Burst and Triensient Source Experiment (BATSE) light curves of long gamma-ray bursts (GRBs) by matched filtering, consistent with a viscous time-scale, and identify ultra-high energy cosmic rays (UHECRs) about the Greisen–Zatsepin–Kuzmin (GZK) threshold with linear acceleration of ion contaminants along the black hole spin-axis, consistent with black hole masses and lifetimes of Fanaroff–Riley type II (FR II) active galactic nuclei (AGN). We explain the absence of UHECRs from BL Lac objects due to UHECR emissions preferably at appreciable angles away from the black hole spin-axis. Black hole spin may be the key to unification of GRBs and their host environments, and to AGN and their host galaxies. Our model points to long-duration bursts in radio from long GRBs without supernovae and gravitational waves from all long GRBs.

Key words: black hole physics – gravitational waves – galaxies: active – gamma-rays: bursts – gamma-rays: observations.

1 INTRODUCTION

Recent developments in high-energy observations reveal a transient Universe abundant in non-thermal emissions across an exceptional range in energies, from radio, as in a recent report on an extragalactic <5 ms radio bursts (Lorimer et al. 2007), to gamma-rays in cosmological gamma-ray burst (GRBs), and ultra-high energy cosmic rays (UHECRs) at energies of 10^{19} eV (Abraham et al. 2007).

Attributing non-thermal emissions and outflows to black holes (BHs) is attractive, as it provides an ideal site for converting gravitational potential energy into various emission channels, by dissipation in an accretion disc or interactions with the spin of the BH. Non-Newtonian behaviour of the radiation processes poses novel observational challenges which may invite novel methods of data analysis and novel probes of the 'physics inside' by neutrino emissions or gravitational waves (Aspera 2008).

Here, we focus on rotating BHs as a potentially common engine to the most energetic non-thermal transient sources. They are described by their mass and angular momentum (generally with a modest electric charge in a state of equilibrium). The outcome may depend on BH spin, and whether accretion discs are sufficiently magnetized to create magnetic outflows. The physical state of nuclei is therefore important to unification schemes of active galactic nuclei (AGN) and quasars (Antonucci 1993; Urry & Padovani 1995; Jackson & Wall 1999) in understanding radio morphologies, continuum and line emissions and, possibly, variability. The Fanaroff–Riley I and II (FR I and FR II, respectively) radio galaxies (Fanaroff & Riley 1974) may serve as an example, possibly with distinctions in the presence or absence of a hidden quasar (Antonocci R., private Communication). The total luminosity alone, however, is sufficient to identify BH spin (Livio, Ogilvie & Pringle 1999).

The Pierre Auger Observatory provides the first angular correlation between UHECRs with nearby AGN in the catalogue of Véron-Cetty & Véron (VCV, 2006). The AGN identified appear to trace nearby spiral galaxies, based on the complete H I Parkes All Sky Survey (HIPASS) (Ghisellini et al. 2008). It might suggest that stellar mass transients or dormant AGN (Levinson 2001) could be the source of the observed UHECRs. However, this does not account for the paucity of UHECRs in the Virgo cluster (Zaw, Farrar & Greene 2008) or the apparent absence of UHECRs with blazars (Harari 2007). The classification of the associated AGN remains tentative, because the VCV catalogue is not complete and may not be an unbiased sample of the AGN Zoology. Based on the combined NASA/IPAC Extragalactic Data base (NED), UHECRs appear to be associated with low-luminosity Seyfert galaxies and LINERs with relatively few radio galaxies (Moskalenko et al. 2008). There may be a minimum bolometric luminosity for UHECRs to unsue, consistent with the paucity of UHECRs from the Virgo cluster (Zaw et al. 2008). UHECRs associated with radio galaxies (Nagar & Matulich 2008) may originate in large radio lobes of FR II AGN (Fraschetti 2008; Fraschetti & Melia 2008). This would require the radio jet to be baryon rich, to account for the observed proton and heavier elements in the UHECRs. It would produce largely

★E-mail: mvp@ligo.mit.edu

isotropic emissions in UHECRs, inconsistent with the paucity of UHECRs from blazars that are hiding FR IIs, and does not account for the apparent association with Seyfert galaxies and LINERs. Instead, UHERs may indeed be produced by some of the galactic nuclei. If confirmed, 'UHECR-active' and 'UHECR-inactive' nuclei promise a significant extension to AGN classification and unification schemes.

In this article, we consider two first-principle physical properties of rotating BHs: a long-duration viscous time-scale of spin-down and ultra-high energy emissions induced by a relativistic capillary effect along the spin-axis (van Putten 2008b):

(i) Exponential decay in the long-duration evolution of GRB light curves, identified by the application of matched filtering to the BATSE catalogue on the premise that the inner engine of long GRBs is long lived (Piran & Sari 1998). The template used is generated by spin-down of a Kerr BH interacting with high-density matter at critical magnetic stability (van Putten & Levinson 2003).

(ii) Creation of UHECRs in a linear accelerator powered by a relativistic capillary effect in the funnel along the spin-axis of the BH surrounded by an ion torus – typical for AGN – with energies that are tightly correlated to the mass of the supermassive BH and the lifetime of the AGN. The latter has recently been studied in some detail for the FR II radio galaxies (O'Dea et al. 2009).

We discuss the application to unification schemes for all GRBs – long and short, with and without supernovae (the *Swift* event GRB 060614; Della Valle 2006; Fynbo et al. 2006; Gehrels et al. 2006; Gal-Yam 2006; Amati et al. 2007) – and UHECR-AGN. We begin with an introduction to the relevant physical properties of Kerr BHs, and apply these to the active nuclei of transient sources. We describe specific observational tests to enable a comparison with observations, present and in the future.

2 SOME PHYSICAL PROPERTIES OF KERR BHS AND SURROUNDING MATTER

Rotating BHs in astrophysical environments introduce at least two unique physical properties: a long-duration time-scale of spin-down associated with a large reservoir in spin energy and linear acceleration to ultra-high energies along their spin-axis.

Rotating BHs (Kerr 1963) are described by their mass M, angular momentum J, specific angular momentum $a = J/M$ and spin energy $E_{\rm s} = \frac{1}{2}\Omega_{\rm H}^2 I f_{\rm s}^2$, where $\sin\lambda = a/M$ (van Putten 1999) with relativistic correction factor $0.7654 < f_{\rm s} = \frac{\cos(\lambda/2)}{\cos(\lambda/4)} < 1$ for the angular velocity $\Omega_{\rm H} = \frac{1}{2M}\tan(\lambda/2)$, and where $I = 4M^3$ denotes the moment of inertia in the limit of slow rotation (Thorne, Price & McDonald 1986). Thus, $E_{\rm s}/M$ can reach 29 per cent ($\lambda = \pm\pi/2$), larger than the spin energy per unit mass in neutron star, by an order of magnitude. Kerr BHs evolve according to the first law of thermodynamics $dM = \Omega_{\rm H} dJ + T_{\rm H} dS$ for changes in spin energy, $dE_{\rm s} = \Omega_{\rm H} dJ$, and dissipation, $dQ = T_{\rm H} dS_{\rm H}$, with the Bekenstein–Hawking entropy (Bekenstein 1973; Bardeen, Carter & Hawking 1973; Hawking 1974; Strominger & Vafa 1996), $S_{\rm H} = 4\pi M^2 \cos^2(\lambda/2)$. In the limit of viscous spin-down with no radiation, we note that $S_{\rm H}$ *doubles* in spin-down to zero from an initial state of maximal spin.

Frame-dragging creates *linear acceleration* by coupling of the Riemann tensor to the angular momentum J of charged particles along open magnetic flux tubes about the spin-axis of a BH. In geometrical units, the product of the Riemann tensor ($\rm cm^{-2}$) and angular momentum ($\rm cm^2$) is of one dimensionless, which represents a force (Papapetrou 1951). Integration along a semi-infinite line to infinity produces a potential energy. In Boyer–Lindquist coordinates, we have, along the spin-axis of the BH (van Putten 2000, 2005, 2008b),

$$\mathcal{E}(r) = \int_r^\infty \text{Riemann} \times J \, {\rm d}s = \omega J. \tag{1}$$

The ensuing *relativistic capillary effect* extracts $e^\pm$-pairs from the environment of the BH, where they are created by canonical pair-cascade processes (Blandford & Znajek 1977), out to larger distance along the spin-axis (van Putten 2000). A transition to a nearly force-free state (Blandford & Znajek 1977) terminates in an outgoing Alfvén front. Thus, the raw Faraday-induced horizon potential (1) is communicated to the outgoing Alfvén front. Since magnetic flux surfaces *upstream* are stable against pair-cascade, they remain largely charge-free, and become clean site for linear acceleration of baryonic contaminants, ionized by exposure to ambient UV-radiation.

In its lowest energy state, the horizon flux Φ^e_θ of a magnetic field with strength B through a polar cap of half-opening angle $\theta_{\rm H}$ is, adapted from (Wald 1974), $\pi B \frac{(r_{\rm H}^2+a^2)^2}{r_{\rm H}^2+a^2\cos^2\theta}\sin^2\theta$, where $r_{\rm H} = 2M\cos^2(\lambda/2)$ and $a = M\sin\lambda$. The full horizon flux ($\theta = \pi/2$) $\Phi^e_{\rm H} = 4\pi BM^2$ is hereby the same for maximal rates and zero-spin, while through a polar cap ($\theta \ll \pi/2$), $\Phi^e_\theta \simeq 2\pi BM^2\theta^2$ about maximal spin (and a factor of 2 larger at zero-spin). The Faraday-induced potential energy on a flux tube with $A_\phi = BM^2\theta^2$ at $r = r_{\rm H}$ in (1) is

$$\mathcal{E}(\theta) = ec\partial_t\Phi = e\Omega_{\rm H}A_\phi \simeq \frac{1}{2}eBM\theta^2 = 2.16\times10^{20}B_5M_9\theta^2{\rm eV} \tag{2}$$

in the limit of maximal spin ($\Omega_{\rm H} \simeq 1/2M$), where $\theta \le \theta_{\rm H}$. The lifetime of spin of a supermassive BH is largely based on dissipation $T_{\rm H}\dot{S}_{\rm H}$ in the event horizon. The average is about one-third of the maximal dissipation rate, i.e.

$$<\dot{Q}> = \frac{c}{3}(\Omega_{\rm H}A_\phi)^2 = \frac{c}{12}B^2M^2 = 5.6\times10^{47}(B_5M_9)^2\,{\rm erg\ s^{-1}}. \tag{3}$$

The lifetime of spin for a maximally spinning BH hereby becomes $T \simeq 29{\rm per\ cent}\times 2\times10^{63}M_9\,{\rm erg}\langle\dot{Q}\rangle^{-1}$, whereby $B_5M_9^{1/2}\,T_7^{1/2} \simeq 1.04$, or

$$B_5M_9 = 1.04\sqrt{\frac{M_9}{T_7}} \tag{4}$$

with $T = T_7\,10^7$ yr following O'Dea et al. (2009). With conservation of flux, $B \simeq 10^5$ G at the ISCO may be compared with $B \sim 10^{-2}$ G fields on sub-parsec scales in Mrk 501 (O'Sullivan & Gabuzda 2008). Scaling to stellar mass BHs surrounded by high-density matter with superstrong magnetic fields gives

$$\langle\dot{Q}\rangle = 6.9\times10^{52}\left(\frac{B}{5\times10^{15}\,{\rm G}}\right)^2\left(\frac{{\rm M}_\odot}{7\,{\rm M}_\odot}\right)^2{\rm erg\ s^{-1}} \tag{5}$$

with

$$\left(\frac{B}{5\times10^{15}\,{\rm G}}\right)\left(\frac{M}{7\,{\rm M}_\odot}\right) = 1.05\sqrt{\frac{M20\ {\rm s}}{7\,{\rm M}_\odot T_{90}}}, \tag{6}$$

where T_{90} refers to the observed durations of long GRBs in seconds.

For the magnetic field strengths in (4) and (6), the mass surrounding the BH can be estimated on the basis of the stability bound for poloidally magnetized discs by van Putten & Levinson (2003)

$$\frac{\mathcal{E}_{\mathcal{B}}}{\mathcal{E}_{\rm k}} \simeq \frac{1}{15} \tag{7}$$

following two closely related models for the poloidal magnetic field of energy $\mathcal{E}_B \simeq \frac{1}{6}B^2R^3$ supported by an inner disc of radius $R_{\rm D}$, mass $M_{\rm D}$ and kinetic energy $\mathcal{E}_{\rm k}$. To leading order, we have $\mathcal{E}_{\rm k} = \frac{GMM_{\rm D}}{2R_{\rm D}}$, so that for supermassive and stellar mass BHs

$$M_{\rm D} \simeq 120\,{\rm M}_\odot \left(\frac{\mathcal{E}_{\rm k}}{15\mathcal{E}_B}\right)\left(\frac{R_{\rm D}}{6R_g}\right)^4\left(\frac{M_9^2}{T_7}\right), \quad (8)$$

$$M_{\rm D} \simeq 0.1\,{\rm M}_\odot \left(\frac{\mathcal{E}_{\rm k}}{15\mathcal{E}_B}\right)\left(\frac{R_{\rm D}}{6R_g}\right)^4\left(\frac{M}{7\,{\rm M}_\odot}\right)^2\left(\frac{20{\rm s}}{T_{90}}\right) \quad (9)$$

with characteristic matter densities of $7.9 \times 10^{-11}\,{\rm g\,cm^{-3}}$ and, respectively, $1.9 \times 10^{11}\,{\rm g\,cm^{-3}}$ (close to the neutron drip line). The associated Alfvén velocities $v_{\rm A}/c = B/\sqrt{4\pi\rho c^2 + B^2}$, where c denotes the velocity of light, are universal, $v_{\rm A}\,[\,{\rm AGN}\,] = 0.1052c$ and, respectively, $v_{\rm A}\,[\,{\rm GRB}\,] = 0.1072\,c$, and are mildly relativistic.

3 GRBS FROM ROTATING BLACK HOLES

Long GRBs represent the complete life cycle of a relativistic inner engine (e.g. Piran & Sari 1998). The recent *Swift* discovery of the long GRB 060614 poses the challenge to identify a common inner engine to long GBRs with and without supernovae.

In suspended accretion, the evolution of a rapidly spinning BH ensues on a viscous time-scale by spin-down against surrounding high-density matter (van Putten 1999; van Putten & Ostriker 2001). The durations of long GRBs are consistent with the lifetime of rapid spin of a BH in interaction with high-density matter at its magnetic stability limit (van Putten & Levinson 2003). This applies to newly born, as in core-collapse (CC) of massive stars (Woosley 1993), or in the binary merger of a neutron star with a companion BH or neutron star. Both scenarios produce a BH torus system (van Putten & Levinson 2003).

We searched for the presence of a viscous time-scale in the GRB light curves of long events in the BATSE catalogue using matched filtering. To this end, we average normalized light curves (nLCs) in durations and count rates, following translations in time, for a best-fit against a template produced by viscous spin-down (equations 7 in van Putten 2008a). We choose the template of an initially extremal black hole, and model its jet-luminosity $L_{\rm j} \propto \Omega_{\rm H}^2 z^2 \mathcal{E}_k$ in the approximation $\mathcal{E}_k \propto (\Omega_{\rm D}R_{\rm D})^2 e(z)$, where $e(z) = \sqrt{1-2/3/z}$ denotes the specific energy of matter with angular velocity $\Omega_{\rm D}$ at the ISCO (Bardeen 1970) and z^2 models a correlation of $\theta_{\rm H}^4$ with $R_{\rm D} = zM$. Fig. 1 shows a comparison of the template with the nLCs of two notable low-variable, low-luminosity events (Reichert et al. 2001). Because these single Fast Rise Exponential Decay (FRED) like light events are rare, we next focus on typical, highly variable light curves from a list of consecutive BATSE triggers, and hence with no selection criteria. Fig. 2 shows some typical fits to the template.

Light curves of GRBs are remarkably diverse, and few look similar. Variability in GRB light curves of long events shows a most variable event, GRB 990510, and least variable events, such as GRB 970508 and GRB 980425, while variability and luminosity are correlated (Reichert et al. 2001). The shortest time-scales of variability reflect intermittency of a long-lived inner engine (Piran & Sari 1998). For GRB-afterglow emissions produced by baryon-poor jets (Shemi & Piran 1990; Frail et al. 2001), variability at intermediate and small time-scales is expected from unsteady radiation processes and modulations by orientation effects, especially for rotationally powered inner engines. An accretion disc or torus is in a state of forced turbulence (van Putten 1999) and may be precessing (Portegies Zwart & McMillian 2000), and their interactions with the central BH should be intermittent, but much less due to time-variability in accretion in the suspended accretion state. Furthermore, the light curves are inherently scaled in energy, photon count rates and durations by their redshifts.

We extract an ensemble average in the form of a nLC, wherein all short time-scale fluctuations have been filtered out relative to the T_{90} of each individual burst by averaging of the individually nLCs

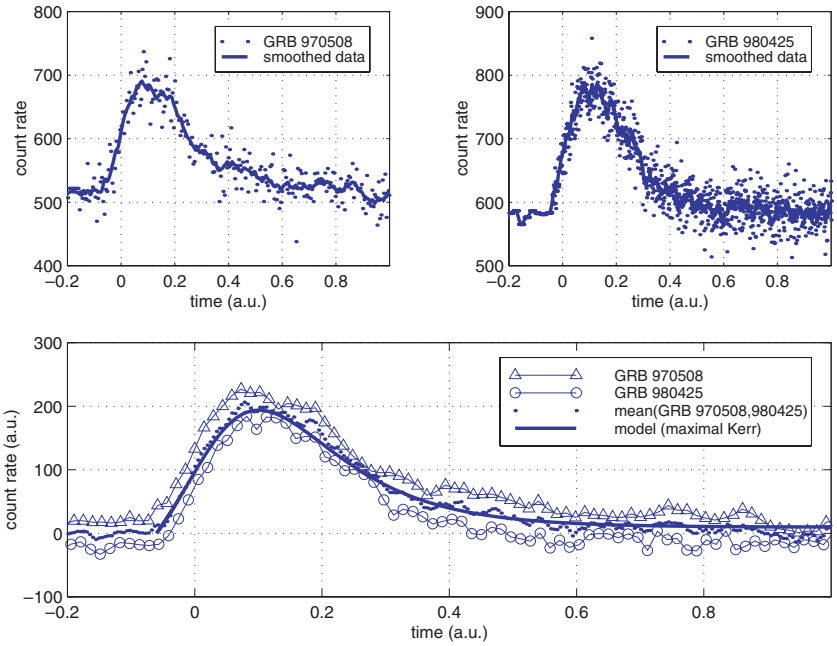

Figure 1. A comparison of two low-variability events, GRB 970508 and GRB 980425, and a template light curve for GRBs from rotating BHs. The two events display a characteristic FRED. The data are scaled in duration and count rate to compare their shape with the template. Note that the true time-of-onset t_0' is slightly before the $t_0 = 0$ in BATSE timing. The GRB light curves have been plotted with a positive and negative offset in normalized count rates for clarity.

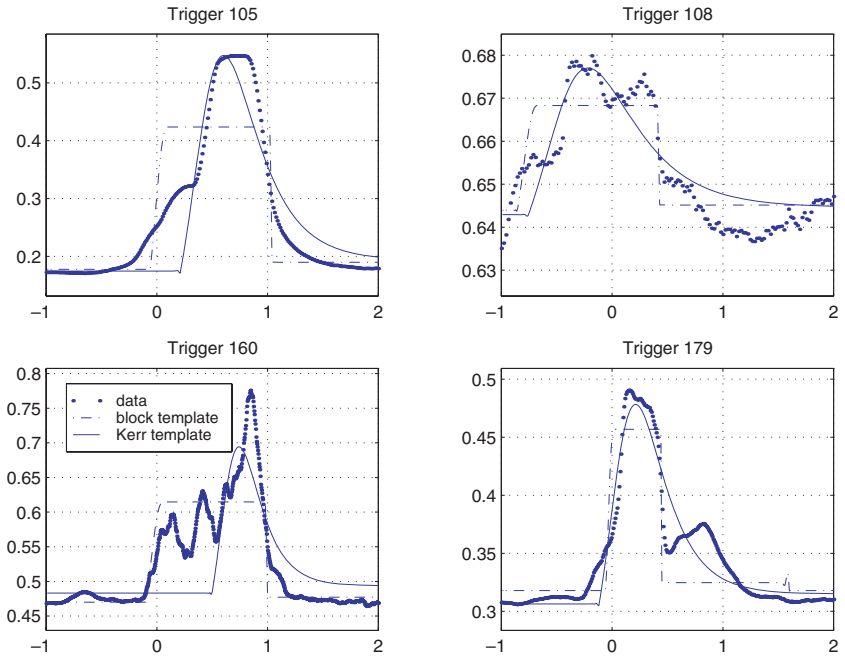

Figure 2. Shown are examples of template fits to various long bursts with normalized durations in the sample L1: $2 < T_{90} < 20$ s, for both the block-type and Kerr templates. In each window, the horizontal axis refers to normalized time (au) and the vertical axis refers to normalized count rates (au). Fitting to a template gives a zeroing of the burst by translations in time defined on the basis of the entire shape of the burst relative to the template, illustrated by Trigger 160, different from using special instants such as the BATSE t_0 data. Light curves are subsequently normalized and averaged to produce a nLC.

against a fixed template. In our procedure, we translate and scale the data to fit a template for producing stable zeroing of the bursts by translation in time followed by normalization to permit taking an ensemble average. It filters out variabilities in the ensemble of light curves at sub-dominant time-scales, and is not focused on studying individual light curves.

Our focus is complementary to the mean spectral properties of GRBs (Fishman et al. 1989), statistics of sub-bursts (Reichert et al. 2001; Quillan et al. 2002), linear temporal profiles in light curves (McBreen et al. 2002a,b) or modelling selected light curves to bright events (Portegies Zwart & McMillian 2000; Lei et al. 2007). Matched filtering is different from earlier approaches based on the BATSE timing signals of the starting time, T_{50}, T_{90} and peak count rates (Mitrofanov et al. 1996; Fenimore 1999). Quite generally, template matching gives stability for burst alignments and scalings, much more so than BATSE timing signals. On this basis, our results disprove the earlier suggestion of a linear decay in the average GRB light curves (Fenimore 1999), which is also not seen in Mitrofanov et al. (1996).

We have verified that our nLC is stable against a choice of template. Fig. 3 shows very similar results obtained for the Kerr template and block-type template (Fig. 3). The matching procedure is consistent, in that block- and Kerr-type templates produce a match of their full width at half-maximum (FWHM), shown in the lower window of Fig. 3. Matched filtering thus creates an nLC as a unique diagnostic for the underlying slow-time behaviour, by filtering out the diversity in GRB light curves due to intermittencies, orientation effects and redshifts.

The exponential decay in the nLC (Fig. 4) is in good agreement with viscous spin-down of Kerr BHs by dissipation of spin energy in the event horizon which, to leading order, represents the creation of an astronomical amount of Bekenstein-Hawking entropy, given an efficiency over the entire process of spin-down of at most 60 per cent and in view of the exceptionally low Hawking temperatures of the horizon of a stellar mass black hole. Thus, entropy is increased by at least 40 per cent of the maximally possible increase

$$S_{\mathrm{H},i} = 2\pi M^2 \rightarrow S_{\mathrm{H},f} = 4\pi M^2, \tag{10}$$

where λ changes from $\lambda_i = \pi/2$ to $\lambda_f = 0$. To the next order, the energetic output of the BH is in various radiation channels by surrounding matter and, to much higher order, in radiation along the spin-axis of the BH.

The GRB afterglow arises by dissipation of the kinetic energy in ultra-relativistic baryon-poor jets in internal and external shocks (Shemi & Piran 1990). Modelling by Poynting flux along an open magnetic flux tube in the force-free limit (Goldrech & Julian 1969; Blandford & Znajek 1977; Thorne et al. 1986) supported by an equilibrium magnetic moment of the BH surrounded by a uniformly magnetized disc or torus predicts a correlation between the peak energy E_{p}, the true energy in gamma-rays E_γ and the durations T_{90} as measured in the local rest-frame, given by (van Putten 2008b)

$$E_{\mathrm{p}} T_{90}^{1/2} \propto E_\gamma, \tag{11}$$

showing a Pearson coefficient of 0.85 in the HETE-II and *Swift* data (Amati et al. 2002; Ghirlanda, Ghisellini & Lazzati 2004; Ghisellini et al. 2007), compiled in fig. 1 of van Putten (2008b).

We attribute the correlation between variability and luminosity (Reichert et al. 2001) to the angular distribution of beamed outflows from open flux tubes with a finite horizon opening angle, consistent with observations (Frail et al. 2001). Their output (luminosity density per steradian) increases with angle between the line-of-sight and the spin-axis of the BH, reaching its maximum along magnetic field lines suspended at a half-opening $\theta_{\mathrm{H}} \sim M/R_{\mathrm{T}}$ on the event horizon set by poloidal curvature in the inner torus magnetosphere,

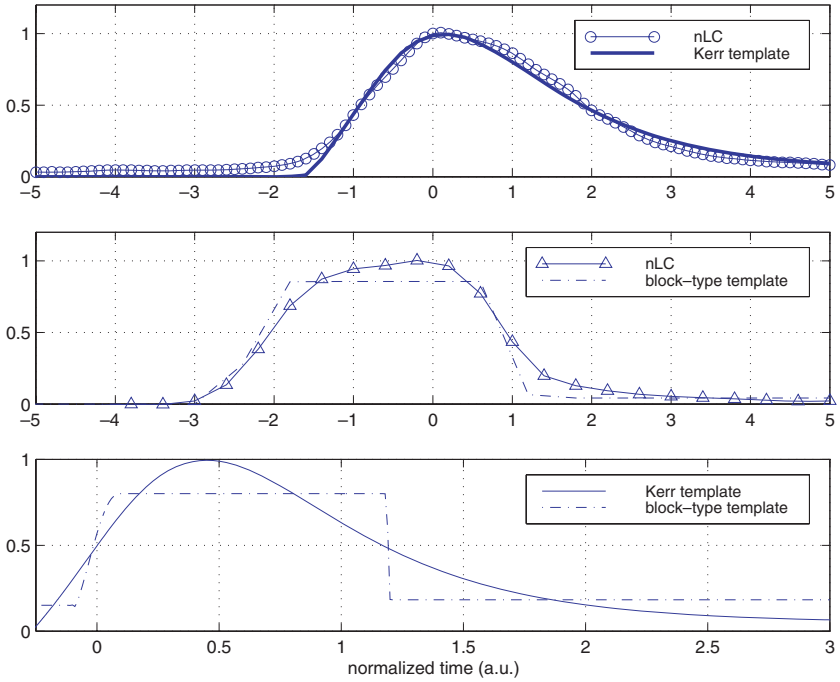

Figure 3. Shown are the nLCs based on a Kerr template and a Kerr-type template for 300 blindly selected long-duration events in sample L1: $2 < T_{90} < 20$ s. In each window, the vertical axis refers to normalized count rates (au). The true nLC has the unique property that it matches its template, which applies to the Kerr (top) but not the block-type template (middle). Note a slightly smoothed average of the block-type templates, due to numerical imperfections in template overlapping. Matching respects the FWHM of the two templates (bottom).

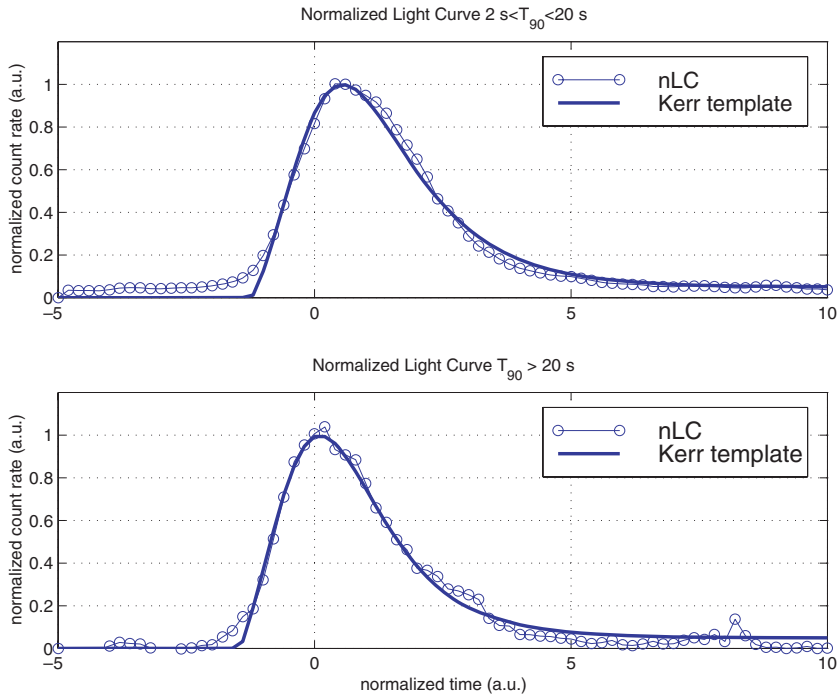

Figure 4. The ensemble average of light curves of long GRBs in the BATSE catalogue is the nLC, obtained by averaging 300 normalized curves of blindly selected long events in sample L1: $2 < T_{90} < 20$ s (top) and 300 blindly selected long events in L2: $T_{90} > 20$ s (below). The normalizations are based on matched filtering, here against the theoretical template representing viscous spin-down of a maximally spinning BH. Convergence of the nLC is slower in L2 than in L1, which may be attributed to frequent intermediate periods of quiescence or dead-periods in the actual GRB light curves. The results show excellent agreement between the theory of viscous spin-down, corresponding to the creation of astronomical amounts of the Bekenstein–Hawking entropy of the even horizon. The match between the nLC and the template appears best for L2, consistent with the longest duration GRBs being produced by black holes with the highest spin-rates.

where R_T denotes the radius of the torus (van Putten & Levinson 2003). The relatively small fraction of spin energy thus released in true energy in gamma-rays E_γ is in good agreement with the observed estimate of $\sim 10^{51}$ erg (Frail et al. 2001). Conceivably, intrinsic variability in gamma-ray emissions reaches a maximum in the boundary layer with the surrounding baryon-rich torus winds. If so, the *observed* variability and luminosity depend on viewing angle. In the nLC, this orientation effect is effectively averaged out.

4 UHECRS FROM SUPERMASSIVE ROTATING BLACK HOLES

The funnel within an ion torus creates a natural environment for an open magnetic flux tube along the spin-axis of the BH, supported by an equilibrium magnetic moment of the BH when exposed to a surrounding magnetic fields (van Putten 1999). The magnetic field may be intermittent in strength and sign, provided it carries a net poloidal magnetic flux.

A relativistic capillary effect induced by differential frame-dragging acting on open magnetic flux tubes introduces a linear accelerator upstream of an outgoing Alfvén front illustrated in Fig. 5. Exposure to UV-radiation from an ion torus in AGN (Ford et al. 1994) allows for acceleration of ionic contaminants to UHECR energies correlated with the physical properties of the central BH.

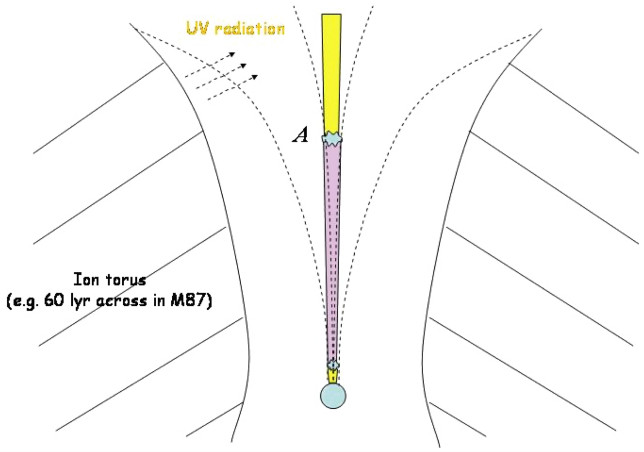

Figure 5. The coupling of the Riemann tensor and angular momentum of charged particles creates a relativistic capillary effect, whereby pairs are extracted from the vicinity of the BH to large distances. The outflow becomes largely force-free up to an outgoing Alfvén front A, which mediates a Faraday-induced horizon Fermi level to large distances along equipotential magnetic flux surfaces. Upstream of A, the magnetic flux surfaces are essentially charge-free, and stable against pair-cascade at large distances from the BH. (Here, frame-dragging is negligible, as it decays with the cube of the distance from the BH.) As ions are produced from stray particles by exposure from UV-radiation from an ion torus, as in the 60 light-year diameter torus of M87, they are subject to linear acceleration by the generating voltages at the Alfvén surface (which are increasing with poloidal angle away from the polar axis). The linear accelerator here forms in particular to intermittent sources, on a time-scale less than the crossing time of the radius of the ion torus. Here, the BH is spun-down against its surroundings (equation 8) not shown) which operates intermittently via an inner torus magnetosphere equivalent in poloidal topology to pulsar magnetospheres (fig. 2 in van Putten 1999).

Based on (2) and (4), we have

$$\mathcal{E} = 5.6 \times 10^{19} \sqrt{\frac{M_9}{T_7}} \left(\frac{\theta_H}{0.5}\right)^2 \text{ eV}, \tag{12}$$

where a horizon half-opening angle $\theta_H \simeq 30^\circ$ is used as a fiducial value based on M87 (Junor, Biretta & Livio 1999; M87, however, is a FR I source). The underlying magnetic field energy – which is currently not accessible to direct observations – is here replaced by its correlation to the lifetime of BH spin, and its identification with the lifetime of FR II radio galaxies. The correlation (12) is in good agreement with the GZK threshold energy of 6×10^{19} eV for observing UHECRs from nearby AGN.

UHECRs may be powerful probes of spin of supermassive BHs. In our model, the UHECRs are emitted anisotropically preferentially along a finite angle relative to the spin-axis of the BH, as in gamma-ray emissions from stellar mass BHs discussed in the previous section. This angle may be appreciable, perhaps as large as 30° on the basis of the opening angle in M87. This picture is consistent with the absence of an UHECR association to BL Lac objects (Harari 2007), which are believed to include both FR I and II sources viewed close to the line-of-sight – too close perhaps for producing UHECRs.

The maximum luminosity L_j of the baryon-poor jet along an open magnetic flux tube can be estimated in terms of the fraction $\sim \frac{3}{8} \sin^4 \theta_H$ of $\langle \dot{Q} \rangle$,

$$L_j = L_- + L_+ \simeq 1.3 \times 10^{46} \left(\frac{M_9}{T_7}\right) \left(\frac{\theta_H}{0.5}\right)^4 \text{ erg s}^{-1}, \tag{13}$$

where L_- may drive dissipation in shocks downstream and L_+ may generate ultra-high energy emissions upstream. Here, L_+ depends on the efficiency of mediating the Faraday-induced horizon potential to the outgoing Alfvén front: it reaches 100 per cent in the force-free limit envisioned by Blandford & Znajek (1977) when $L_- \simeq 0$. The luminosity in UHECRs depends on the density of ionic contaminants upstream, and their exposure to UV radiation. The observed time-averaged AGN luminosity, considered in Waxman (2004), is here governed by the time-averaged $\langle \theta_H^4(t) \rangle$, which does not provide a sharp constraint on peak energies in UHECRs. Geometrical considerations suggest $\langle \theta_H^4(t) \rangle \propto \langle R_D^2(t) \rangle^2 / M^2$ is set by a time-variable disc radius $R_D(t)$, as in the Seyfert galaxy MCG 60-30-15 (Tanaka, Nandra & Fabian 1995; Iwasawa et al. 1996). Including the duty cycle, $\langle L_j(t) \rangle$ can hereby be smaller than the peak values (13) by 1 to 2 orders of magnitude. Low-luminosity AGN hereby favour UHECR production by allowing for relatively clean sites for particle acceleration. In light of (13), it would therefore be of interest to pursue an observational study of the true ages of Seyfert galaxies. See further (van Putten & Wilson 1999; Farrar & Gruzinov 2008) for related considerations on intermittencies.

In general, therefore, (13) is an upper limit to a luminosity in UHECRs which may be intermittent on time-scales of the light-crossing time of the ion torus – tens of years or less – and extending for the lifetime of spin of the BH, i.e. 1–10 million years, on the basis of observational lifetimes of FR II radio galaxies.

The same principles apply to UHECRs from spinning stellar mass BHs in GRBs. Expressed in total energy output, the relative contributions to the PAO observations satisfy

$$\frac{\mathcal{E}[\text{GRB}]}{\mathcal{E}[\text{AGN}]} \simeq 1.4 \times 10^{-4} \left(\frac{N[\text{AGN}, < 100 \text{ Mpc}]}{500}\right)^{-1}, \tag{14}$$

given 1 long GRB yr^{-1} within 100 Mpc and scaled against a fiducial number of 500 AGN powered by BH spin within this distance. GRBs appear to be sub-dominant.

5 CONCLUSIONS AND OUTLOOK

The findings in this paper are part of a study on durations, light curves, spectral properties and correlations to the mass and lifetime of BH spin.

(1) We identify the bi-modal distribution of durations in the BATSE catalogue with hyper- and suspended accretion on slowly and rapidly spinning BHs (equations 7, 8 and 9, respectively, in van Putten & Ostriker 2001). The time-scale of hyperaccretion on to slowly spinning BHs is $\sim t_{\rm ff}\mathcal{E}_{\rm k}/\mathcal{E}_B \simeq$ tenth of seconds, where $t_{\rm ff}$ denotes the free-fall time-scale. BH angular velocities that are slower and faster than the angular velocity at the ISCO thus give rise to transient sources to the left and, respectively, to the right of the break at $\sim$2 s separating the two classes in the BATSE catalogue. Unification on the basis of BH spin rates predicts low-luminosity X-ray afterglows also to short GRBs (van Putten & Ostriker 2001), confirmed by *Swift* in GRB 050709 and HETE II in GRB 050509B. This unification does not require (but does not rule out) different values of the magnetic field strength and the mass of the BH.

(2) We report on an exponential decay in the BATSE catalogue of light curves of long GRBs in agreement with viscous spin-down of a Kerr BH. The quality of the fit to the model template by matched filtering shows that long GRBs are to leading order a process of doubling the entropy of the event horizon, expressed in (10).

(3) We describe a common inner engine to unify long events GRB 030329/SN2003h and GRB 060614 with and without supernovae, produced in CC SNe (Woosley 1993; Paczynski 1998) and the binary merger of a neutron star with a rapidly spinning BH (van Putten 1999) or a companion neutron star (fig. 1 in van Putten & Levinson 2003).

(4) Our model predicts a spectral-energy correlation (11) in agreement with HETE II and *Swift* data with a Pearson coefficient of 0.85 (fig. 1 in van Putten 2008b).

(5) Our model predicts UHECRs with energies (12) correlated to the mass of the central BH and the lifetimes of AGN in agreement with PAO data, and emitted anisotropically consistent with the paucity of UHECRs from BL Lac objects.

For GRBs, accretion-powered models (e.g. Woosley 1993; Kumar, Narayan & Johnson 2008) are different. They do not account for GRB 060614, since it was not a CC event (Della Valle et al. 2006). Winds from the inner disc, at typical temperatures of 1–2 MeV, are too contaminated to produce the ultra-relativistic (baryon-poor) outflows needed to account for the observed GRB-afterglow emissions and spectral-energy correlations. If attributed to the central BH, then its spin *up* by continuing accretion (Kumar et al. 2008) is at odds with the decay in BATSE data (Fig. 1).

Late-time X-ray emissions on a time-scale of 1–10 ks – distinct from X-ray afterglows to the prompt GRB emissions – are observed by *Swift* in a number of long GRBs (see Zhang 2007 for a review). They can be attributed to late-time infall of the outer envelope of a remnant progenitor star in CC events (Kumar et al. 2008). Late-time infall on to a BH, regardless of spin, may be expected to be luminous as matter forms high densities in the process of free fall (as in SN1987A). In the absence of a massive progenitor star, as in mergers of a neutron star and a BH or mergers of two neutron stars, we anticipate that events such as GRB 060614 – and more generally long GRBs with anomalously low-luminosity X-ray afterglow emissions, identified with binary mergers in low-density environments – feature no or relatively weak late-time X-ray emissions. Weak late-time X-ray emissions are expected, since the break-up of the neutron star(s) in a binary merger is known to be potentially messy, leaving matter at relatively large radii to fall in with appreciable time delay. This may be verified observationally, by searching for late-time X-ray emissions in long GRBs without supernovae and GRBs – long and short – with anomalously low X-ray afterglows to their prompt GRB emissions.

To illustrate our unification scheme, we interpret some pivotal GRBs as follows.

GRB 050709, GRB 050509B (*short GRBs with X-ray afterglows*). Binary mergers of a neutron star with a slowly spinning BH, producing a short-duration event in a state of hyperaccretion. The weak GRB afterglows were produced by BH outflows, interacting with a low-density environment typical for binaries.

GRB 030329 (*long GRB-supernova*). CC of a massive star, producing a long-duration event in a state of suspended accretion. GRB afterglow emissions were produced by BH outflows from a rapidly spinning BH, interacting with high-density environments typical for star-forming regions.

GRB 050911 (*long GRB without X-ray afterglow*). The binary coalescence of a neutron star with a rapidly spinning BH or the merger of two neutron stars, giving rise to a long-duration event in a state of suspended accretion. The absence of a negotiable X-ray afterglow is attributed to an exceptionally low-density environment of the progenitor binary.

GRB 060614 (*long GRB without supernova*). Binary coalescence of a neutron star with a rapidly spinning BH or the merger of two neutron stars, giving rise to a long-duration event in suspended accretion without a supernova. The relatively low luminosity X-ray plateau is attributed to a limited amount of late-time infall of remnant matter following the break-up of the neutron star(s).

GRB 070110 (*long GRB with late-time X-ray emissions*). A CC of a massive star GRB-supernova with late-time X-ray emissions from fall-back of matter from the remnant stellar envelope (Kumar et al. 2008).

GRB 080319B (*luminous and variable long GRB*). A GRB viewed along the boundary of a baryon-poor jet, where the luminosity and variability are highest subject to instabilities in interaction with surrounding baryon-rich disc winds.

If GRBs and the recently reported short-duration radio burst (if confirmed) are related, then long-duration radio bursts may exist associated with events like GRB 060614 or, more generally, with long-duration bursts with anomalously weak X-ray afterglows.

Complete optical-radio surveys of the local transient universe promise to provide a valuable catalogue of CC supernovae, radio-loud SNe and radio bursts. These surveys can be optimized by scanning along the local super-clusters, avoiding the large-area voids in between (Einasto et al. 1994). They may be augmented by large neutrino detectors (Shin'ichiro, Beacom & Hasan 2005) to provide real-time triggers of the onset of supernovae as in SN1987A. The Australian MOST survey illustrates surveys of radio-loud SNe, all of which are CC SNe, few of which will be associated with long GRBs in view of a branching ratio of a mere 0.2–0.4 per cent of Type Ib/c into GRBs (van Putten 2004). Augmented by optical surveys, e.g. by Pan-STARRs (in the Northern Hemisphere), these surveys could provide targets of interest to the Laser-Interferometric Gravitational-wave Observatory (LIGO) and VIRGO, to study a possibly common inner engine to Type II and Type Ib/c SNe, perhaps similar to those at work in GRBs, the latter which are expected to have a long-duration bursts in gravitational waves with negative chirp. The CC-SNe scenario for long GRB SNe requires a companion star in close binary orbit to ensure rapid rotation by tidal interaction (Paczynski 1998). At present, a companion has only

been identified to the Type II/Ib SN 1993J event (Maund et al. 2004), otherwise not known to have been a GRB.

The FR I and II classification expresses a dichotomy in radio galaxies (Fanaroff & Riley 1974), as in 3C31 and Pic A. The FR II sources are lobe-dominated and edge-brightened, straight and one-sided (on the kpc scale), which is testimony to their power, exceptional long-term orientation stability and radiation beaming in relativistic outflows. It suggests that FR IIs may be associated with BH spin, more likely so than the probably accretion-powered FR Is (Baum, Zirbel & O'Dea 1995). But, the FR IIs may not be the only AGN harbouring rapidly spinning BHs. Follow-up PAO statistics on UHECRs will be important in confirming the association with AGN, and in identifying the type of AGN, host galaxies and their orientation relative to the line-of-sight. We suggest that spinning BHs may be hosted in Seyferts and LINERs, producing largely leptonic outflows and emissions in UHECRs without baryon-rich disc winds. UHECR-AGN without FR II morphology may be understood by the absence of disc winds, perhaps due to weak poloidal magnetic fields. When radio jets do form, polarization studies on FR I and II jets show large-scale-ordered magnetic fields with more pronounced toroidal magnetic fields in FR II sources. BH spin interacts largely with the inner disc, through the *time-average* of energy density of net poloidal magnetic flux, while the UHECR production is associated with *instantaneous* poloidal magnetic flux along an open flux tube with finite opening angle set by a generally time-variable radius of the inner disc. The outflows will remain largely baryon-free in the absence of outer disc winds (cf. the X-ray jet of the Crab pulsar; Lu et al. 2001), inhibiting dissipation in shocks to re-accelerate charged particles (cf. modelling GRB afterglows; Shemi & Piran 1990). There may therefore be anomalously weak or unseen extended radio emissions associated with intermittent UHECR production from clean sites for acceleration in Seyfert galaxies, where the details may be constraint by the lifetime of Seyfert galaxies.

ACKNOWLEDGMENTS

We thank the referee for a number of thoughtful comments and Ski Antonucci for stimulating discussions. This work is supported, in part, by a grant from the Région Centre of France.

REFERENCES

Abraham J. et al. (Pierre Auger Collaboration), 2007, Sci, 318, 938
Amati L. et al., 2002, A&A, 390, 81A
Amati L., Della Valle M., Frontera F., Malesani D., Guidorzi C., Montanari E., Pian E., 2007, A&A, 463, 913
Antonucci R., 1993, ARA&A, 31, 473
ASPERA ERANET, Roadmap of Astroparticle Physics, http://brussels2008.aspera-eu.org
Bardeen J. M., 1970, Nat, 226, 64
Bardeen J. M., Carter B., Hawking S. W., 1973, Commun. Math. Phys., 31, 161
Baum S. A., Zirbel E. L., O'Dea C. P., 1995, ApJ, 451
Bekenstein J. D., 1973, Phys. Rev. D, 7, 2333
Blandford R. D., Znajek R. L., 1977, MNRAS, 179, 433
Della Valle M. et al., 2006, Nat, 444, 1050
Einasto M., Einastro J., Tago E., Dalton G. B., Andernach H., 1994, MNRAS, 269, 301
Fanaroff B. L., Riley J. M., 1974, MNRAS, 167, 31P
Fenimore E. E., 1999, ApJ, 518, 375
Farrar G. R., Gruzinov A., 2008, preprint (arXiv:0802.1074)
Ford H. C. et al., 1994, ApJ, 435, L27
Frail et al., 2001, ApJ, 562, L55
Fraschetti F., 2008, Phil. Trans. R. Soc. A., 366, 4417
Fraschetti F., Melia F., 2008, MNRAS, 391, 1100
Fishman G. J. et al., 1989, in Johnson N., ed. Proc. GRO Science Workshop, Vol. 2, NRL, Washington, DC, p. 39
Fynbo J. P. U. et al., 2006, Nat, 444, 1047
Gal-Yam A. et al., 2006, Nat, 444, 1053
Gehrels N. et al., 2006, Nat, 444, 1044
Ghirlanda G., Ghisellini G., Lazzati D., 2004, ApJ, 616, 331
Ghisellini G., Celotti A., Ghirlanda G., Firmani C., Nava L., 2007, MNRAS, 382, L72
Ghisellini G., Ghirlanda G., Tavecchio F., Fraternali F., Pareschi G., 2008, MNRAS, 390, L88
Goldreich P., Julian W. H., 1969, ApJ, 157, 869
Harari D., 2007, in Caballero R., D'Olivo J. C., Medina-Tanco G., Nellen L., Sánchez F. A., Valdés-Galicia J. F., eds, Proc. 30th International Cosmic Ray Conf. Vol. 4. Universidad Nacional Autónoma de México, Mexico City, p. 283
Hawking S. W., 1974, Nat, 248, 30
Iwasawa K. et al., 1996, MNRAS, 282, 1038
Jackson C., Wall J. V., 1999, MNRAS, 304, 160
Junor W., Biretta J. A., Livio M., 1999. Nat, 401, 891
Kerr R. P., 1963, Phys. Rev. Lett., 11, 237
Kumar P., Narayan R., Johnson J. L., 2008, Sci, 321, 376
Lei W. H., Wang D. X., Gong B. P., Huang C. Y., 2007, A&A, 468, 563
Levinson A., 2001, in Aharonian F. A., Völk H. J., eds, Proc. AIP Symp. 558, High Gamma-Ray Astronomy. American Institute of Physics, Melville, New York, p. 798
Livio M., Ogilvie G. I., Pringle J. E., 1999, ApJ, 512, 100
Lorimer D. R., Bailes M., McLaughlin M. A., Narkevic D. J., Crawford F., 2007, Sci, 318, 777
Lu F. J., Aschenbach B., Song L. M., Durouchoux P., 2001, Ap&SS, 276, 141
McBreen S., McBreen B., Hanlon L., Quilligan F., 2002a, A&A, 393, L15
McBreen S., McBreen B., Hanlon L., Quilligan F., 2002b, A&A, 393, L29
Maund J. R., Smartt S. J., Kudritzki R. P., Podsiadiowski P., Gilmore G. F., 2004, Nat, 427, 129
Mitrofanov I. G., Chernenko A. M., Pozanenko A. S., Briggs M. S., Paciesas W. S., Fishman G. J., Meegan C. A., Sagdeev R. Z., 1996, ApJ, 459, 570
Moskalenko I. V., Stawarz L., Porter T. A., Cheung C.-C., 2008, preprint (astro-ph/0805.1260)
Nagar M., Matulich J., 2008, A&A, 488, 879
O'Dea C. P., Daly R. A., Kharb P., Freeman K. A., Baum S. A., 2009, A&A, 494, 471
O'Sullivan S. P., Gabuzda D. C., 2008, Proc. 9th EU VLBI Network Symposium: The Role of VLBI in the Golden Age for Radio Astronomy and EVN Users Meeting, preprint (arXiv:0812.3412)
Paczynski B. P., 1998, ApJ, 494, L45
Papapetrou A., 1951, Proc. R. Soc., 209, 248
Piran T., Sari R., 1998, in Olinto A. V., Friedman J. A., Schramm D. N., eds, 18th Texas Symp. Relat. Astroph. Cosmology, World Scientific, Singapore, p. 34
Portegies Zwart S. F., McMillain S. F. W., 2000, ApJ, 528, L17
Quilligan F., McBreen B., Hanlon L., McBreen S., Hurley K. J., Watson D., 2002, A&A, 385, 377
Reichert D. E., Lamb D. Q., Fenimore E. E., Ramirez-Ruiz E., Cline T. L., Hurley K., 2001, ApJ, 552, 57
Shemi A., Piran T., 1990, ApJ, 365, L55
Shin'ichiro A., Beacom J. F., Hasan Y., 2005, Phys. Rev. Lett., 95, 171101
Tanaka Y., Nandra K., Fabian A. C., 1995, Nat, 375, 659
Thorne K. S., Price R. H., McDonald D. H., 1986, Black Holes: The Membrane Paradigm. Yale Univ. Press, New Haven, CT
Urry C. M., Padovani P., 1995, PASP, 107, 803
van Putten M. H. P. M., 1999, Sci, 284, 115
van Putten M. H. P. M., 2000, Phys. Rev. Lett., 84, 3752
van Putten M. H. P. M., 2004, ApJ, 611, L81
van Putten M. H. P. M., 2005, Nuov. Cim. C, 28, 597
van Putten M. H. P. M., 2008a, ApJ, 684, L91

van Putten M. H. P. M., 2008b, ApJ, 685, L63
van Putten M. H. P. M., Ostriker E. C., 2001, ApJ, 552, L31
M. H. P. M., Levinson A., 2003, ApJ, 584, 937
van Putten M. H. P. M., Wilson A., 1999, http://online.kitp.ucsb.edu/online/bhole_c99/
Wald R. M., 1974, Phys. Rev. D., 10, 1680
Waxman E., 2004, Pramana, 62, 483
Véron-Cetty M.-P., Véron P., 2006, A&A, 455, 773
Woosley S. L., 1993, ApJ, 405, 273
Zaw I., Farrar G. R., Greene J. E., 2008, preprint (arXiv:0806.3470)
Zhang B., 2007, Adv. Space Res., 40, 1186

This paper has been typeset from a TEX/LATEX file prepared by the author.